



Contents lists available at ScienceDirect

## Journal of Colloid and Interface Science

www.elsevier.com/locate/jcis



## Fullerene oxidation and clustering in solution induced by light



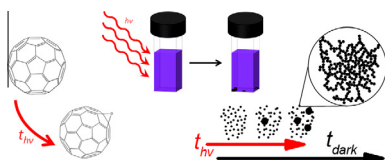
Rajeev Dattani<sup>a,b</sup>, Kirsty F. Gibson<sup>b</sup>, Sheridan Few<sup>a,c</sup>, Aaron J. Borg<sup>b</sup>, Peter A. DiMaggio<sup>b</sup>, Jenny Nelson<sup>a,c</sup>, Sergei G. Kazarian<sup>b</sup>, João T. Cabral<sup>a,b,\*</sup>

<sup>a</sup> Centre for Plastic Electronics, Imperial College London, London SW7 2AZ, United Kingdom

<sup>b</sup> Department of Chemical Engineering, Imperial College London, London SW7 2AZ, United Kingdom

<sup>c</sup> Department of Physics, Imperial College London, London SW7 2AZ, United Kingdom

## GRAPHICAL ABSTRACT



## ARTICLE INFO

## Article history:

Received 24 November 2014

Accepted 5 January 2015

Available online 22 January 2015

## Keywords:

Fullerene  
Aggregation  
Light exposure  
Oxidation  
C<sub>60</sub>  
Epoxide

## ABSTRACT

We investigate the environmental stability of fullerene solutions by static and dynamic light scattering, FTIR, NMR and mass spectroscopies, and quantum chemical calculations. We find that visible light exposure of fullerene solutions in toluene, a good solvent, under ambient laboratory conditions results in C<sub>60</sub> oxidation to form fullerene epoxides, and subsequently causes fullerene clustering in solution. The clusters grow with time, even in absence of further illumination, and can reach dimensions from  $\approx 100$  nm to the  $\mu\text{m}$  scale over  $\approx 1$  day. Static light scattering suggests that resulting aggregates are fractal, with a characteristic power law ( $d_f$ ) that increases from approximately 1.3 to 2.0 during light exposure. The clusters are bound by weak Coulombic interactions and are found to be reversible, disintegrating by mechanical agitation and thermal stress, and reforming over time. Our findings are relevant to the solution processing of composites and organic photovoltaics, whose reproducibility and performance requires control of fullerene solution stability under storage conditions.

© 2015 The Authors. Published by Elsevier Inc. This is an open access article under the CC BY license (<http://creativecommons.org/licenses/by/4.0/>).

## 1. Introduction

Since the advent of large scale fullerene production [1], photo-polymerisation and -oxidation has been reported for C<sub>60</sub> fullerenes and their derivatives in the solid state [2] and is now relatively well understood [2–5]. By contrast, the environmental stability of fullerene solutions, despite its relevance for plastic electronics [6]

and fullerene-based composites [7], has received comparatively less attention. Three outcomes have been reported for the light exposure of C<sub>60</sub> solutions: degradation of the fullerene cage [8,9], photo-polymerisation [10] and oxidation [10] whilst others have reported aggregation with considering light exposure [11–15].

Degradation of the fullerene cage (photolysis) has been found by UV radiation in hexane [8,9], eventually leading to the formation of a brown deposit which could not be re-dissolved [8]. Fullerene photo-polymerisation and -oxidation upon UV exposure has been investigated in a variety of chlorinated and saturated hydrocarbon solvents, in ambient and inert atmospheres [10]. UV light was found to cause photo-oxidation in saturated hydrocarbon solvents and ambient conditions, while fullerene photo-polymerisation was reported to occur in chlorinated solvents in inert

\* Corresponding author at: Department of Chemical Engineering, Imperial College London, London SW7 2AZ, United Kingdom.

E-mail addresses: [rajeev.dattani10@imperial.ac.uk](mailto:rajeev.dattani10@imperial.ac.uk) (R. Dattani), [kgibson@imperial.ac.uk](mailto:kgibson@imperial.ac.uk) (K.F. Gibson), [sheridan.few10@imperial.ac.uk](mailto:sheridan.few10@imperial.ac.uk) (S. Few), [a.borg12@imperial.ac.uk](mailto:a.borg12@imperial.ac.uk) (A.J. Borg), [p.dimaggio@imperial.ac.uk](mailto:p.dimaggio@imperial.ac.uk) (P.A. DiMaggio), [j.nelson@imperial.ac.uk](mailto:j.nelson@imperial.ac.uk) (J. Nelson), [s.kazarian@imperial.ac.uk](mailto:s.kazarian@imperial.ac.uk) (S.G. Kazarian), [j.cabral@imperial.ac.uk](mailto:j.cabral@imperial.ac.uk) (J.T. Cabral).

atmosphere. The formation of a brown deposit was then rationalised as arising from fullerene ‘polymer’. Similar UV spectroscopy data at wavelengths of 330 and 400 nm has, however, been interpreted as either evidence of decomposition [9,8] or polymerisation [10]. Discriminating between these results appears thus difficult via UV spectroscopy, and both fullerene degradation and photopolymerisation remain rather poorly understood.

Although fullerene aggregation in solution has been previously reported [11,12,15,13,14], its trigger and mechanism have not yet been elucidated. Ying et al. [11,12] studied fullerene/benzene solutions over a 40–90 day period using static and dynamic light scattering. An increase in scattering intensity over time was found, which was reversed upon hand shaking the solution. A laser wavelength of 790 nm (and power of 30 mW) was assumed to be sufficiently away from the UV region in which degradation or polymerisation had been reported to occur, although fullerene oxidation is likely to take place close to this wavelength range [16]. Solution storage between measurements, in terms of light exposure and solution atmosphere, was not discussed but the formation of an insoluble brown residue was also observed. All solution concentrations in the above studies were below the reported solubility limits [17] and agglomeration was thus not expected. Mixed solvent systems containing toluene and acetonitrile [14] or aqueous electrolyte solutions [15] have been found to cause C<sub>60</sub> cluster formation and crystallisation with various crystal symmetries [18], but are beyond the scope of the present study.

Several mechanisms can potentially describe fullerene aggregation, according to rate limiting factors and fractal geometry. Generally, these include reaction-limited and diffusion-limited aggregation and, within these, models for monomer–cluster and cluster–cluster aggregation [19]. Reaction-limited aggregation has typical energy barriers of  $\approx 10 k_B T$  [20] which must be overcome for aggregation to occur, whereas diffusion-limited aggregation is effectively barrier-less and the aggregation process is limited by the cluster diffusion. A characteristic fractal power law ( $d_f$ ) found from an elastic scattering experiment  $I \propto q^{-d_f}$ , where  $q$  is wavenumber, distinguishes the two regimes as both yield characteristic structures. Reaction-limited monomer–cluster aggregation, otherwise known as the Eden model [21] and diffusion-limited monomer–cluster aggregation [22] both result in more compact structures, characterised by a higher  $d_f$  of 3 and 2.5 respectively, compared to their cluster–cluster analogues [19]. A ‘poisoned’ Eden model [23,24] describes the aggregation of primary particles that are not only limited by a reaction step, but also by a limited number of possible sites where aggregation can take place. A crossover from reaction-limited to diffusion-limited mechanisms can also be expected [25,20], as the growing clusters become increasingly hindered diffusion through the solvent, as opposed to the sticking probability between individual particles. This mechanism predicts a decreasing  $d_f$  as agglomeration proceeds, typically from 2.1 to 1.8 [25].

In this work, we probe the light-induced oxidation and subsequent clustering of C<sub>60</sub> in toluene via static and dynamic light scattering alongside analytical techniques and computational calculations of the factors governing fullerene association.

## 2. Materials and methods

Neat C<sub>60</sub> fullerenes (99% MER Corp) were dissolved in toluene (99.5%, VWR), at various concentrations below the reported miscibility limit (0.32 wt%) [17]. All solution vials were wrapped in aluminium foil to minimise ambient light exposure prior to controlled light exposure. Four light sources were evaluated, specifically: a 633 nm, 4 mW, HeNe laser, a 100 W, Mercury UV-A (365 nm) lamp, a high intensity white light, and ambient laboratory light

(detailed in Section S3). The most effective light source was found to be the red laser source, with the highest irradiance, and was thus employed for most experiments reported in this study. Exposure times ranged from 0 to 25 h in a 1 cm rectangular quartz cuvette (Hellma) sealed with PTFE tape and a screw-top lid to prevent evaporation. All experiments were carried out with 1 ml of solution at 25 °C, unless otherwise specified. Prior to measurements the C<sub>60</sub>/toluene solutions were filtered through a 220 nm PTFE filter (VWR) to remove dust and particulates. Dynamic Light Scattering (DLS) was performed in the same cuvette using a Malvern Nano-S with a fixed angle detector at  $\theta = 173^\circ$ , corresponding to  $q = 2.96 \times 10^{-2} \text{ nm}^{-1}$ , where  $q = \frac{4\pi n}{\lambda} \sin \frac{\theta}{2}$ , and  $n$ ,  $\lambda$  and  $\theta$  are the refractive index of the solvent (1.496), laser wavelength (633 nm) and scattering angle ( $173^\circ$ ) respectively. The field correlation function  $g^{(1)}(t)$  obtained from DLS was fit with a series of exponentials using<sup>1</sup>:

$$g^{(1)}(t) = \sum_{i=1}^N a_i(q) \exp(-\Gamma_i t) \quad (1)$$

where  $a_i$  is the scattering amplitude of the  $i$ th mode, and  $\Gamma_i$  is the mean inverse relaxation time of each diffusive mode, with  $N \leq 3$ . The diffusion coefficient  $D_i$  of each mode is computed from  $\Gamma_i = D_i q^2$  and the hydrodynamic radius,  $R_{h,i}$ , of the particles is obtained from the Stokes–Einstein equation:

$$R_{h,i} = \frac{k_B T}{6\pi\eta D_i} \quad (2)$$

where  $k_B$  is the Boltzmann constant,  $T$  is the temperature and  $\eta$  is the dynamic viscosity of the solvent, for toluene ( $5.5 \times 10^{-4} \text{ Pa s}$  for toluene at 25 °C). In order to reproducibly fit the various decay modes, the fastest decay ( $\Gamma_1$ ) was fixed, as it is present in neat toluene as well as fullerene solutions and cannot be interpreted quantitatively. A contribution from molecular C<sub>60</sub>, expected at the nanosecond time scale is not resolved reliably, likely due to its low content in solution (bound by its low miscibility in toluene) and limited detector sensitivity. The second decay ( $\Gamma_2$ ) was assigned to clusters which form upon illumination with dimensions  $R_{h,2}$  of the order of 100 nm. The final decay ( $\Gamma_3$ ) yields  $R_{h,3}$  on the order of 10  $\mu\text{m}$ , beyond the limit of Brownian diffusion analysis. It is common for long decay times detected by DLS, corresponding to particulates of dimensions on the order of 10  $\mu\text{m}$ , to be ascribed to contaminants; however, due to the trend observed during light exposure, and their initial absence in the filtered solution, we interpret them as large C<sub>60</sub> clusters. These larger particles can eventually be observed in solution via transmission optical microscopy (Olympus BX71), confirming the formation of large clusters of 10–90  $\mu\text{m}$  dimensions. The amplitude of each mode,  $a_1$ ,  $a_2$  and  $a_3$  is also computed, quantifying their relative population. The three modes, characteristic  $R_{h,i}$ , and attributed physical meaning are summarised in Table 1. Mass spectroscopy (LTQ Velos Pro, Thermo Scientific), FTIR (Bruker Tensor 27) and NMR (Av500) spectroscopies were used to characterise light exposed C<sub>60</sub> solutions. Quantum chemical calculations were carried out on pairs of C<sub>60</sub>O<sub>x</sub> molecules. Further details of these analytical techniques, computational methods and sample preparation can be found in Section S1.

<sup>1</sup>  $\Gamma_i$  is the mean inverse relaxation time of diffusive modes with the z-averaged translational diffusion coefficient  $D_i = \Gamma_i / q^2$ . For the case of two or three well-separated modes, DLS data can be adequately modeled with double- or triple-exponentials ( $N = 2$  or  $3$ ). This allocates one exponential per mode and hence allows for a statistically robust estimate of the z-averaged particle size and of the corresponding partial scattering intensity of the respective mode.

Download English Version:

<https://daneshyari.com/en/article/6996950>

Download Persian Version:

<https://daneshyari.com/article/6996950>

[Daneshyari.com](https://daneshyari.com)